Bioactive Materials 35 (2024) 259–273

Contents lists available at ScienceDirect

Bioactive Materials

journal homepage: www.keaipublishing.com/en/journals/bioactive-materials

Wet environment-induced adhesion and softening of coenzyme-based polymer elastic patch for treating periodontitis

Ying Qi [a,1], Chenyu Xu [b,1], Zhuodan Zhang [a], Qian Zhang [a], Ziyang Xu [a], Xinrui Zhao [a], Yanhong Zhao [b,**], Chunyan Cui [a,***], Wenguang Liu [a,*]

[a] School of Materials Science and Engineering, Tianjin Key Laboratory of Composite and Functional Materials, Tianjin University, Tianjin, 300350, China
[b] School and Hospital of Stomatology, Department of Orthodontics, Tianjin Medical University, Tianjin, 300070, China

ARTICLE INFO

Keywords:
Co-enzyme
α-Lipoic acid
Wet tissue adhesion
Elastic patch
Periodontitis

ABSTRACT

Periodontitis, a common chronic inflammatory disease caused by pathogenic bacteria, can be treated with diverse biomaterials by loading drugs, cytokines or proteins. However, these biomaterials often show unsatisfactory therapeutic efficiency due to their poor adhesion, short residence time in the wet and dynamic oral cavity and emerging drug resistance. Here we report a wet-responsive methacrylated gelatin (GelMA)-stabilized coenzyme polymer poly(α-lipoic acid) (PolyLA)-based elastic patch with water-induced adhesion and softening features. In PolyLA-GelMA, the multiple covalent and hydrogen-bonding crosslinking between PolyLA and GelMA prevent PolyLA depolymerization and slow down the dissociation of PolyLA in water, allowing durable adhesion to oral periodontal tissue and continuous release of LA-based bioactive small molecule in periodontitis wound without resorting external drugs. Compared with the undifferentiated adhesion behavior of traditional adhesives, this wet-responsive patch demonstrates a favorable periodontal pocket insertion ability due to its non-adhesion and rigidity in dry environment. In vitro studies reveal that PolyLA-GelMA patch exhibits satisfactory wet tissue adhesion, antibacterial, blood compatibility and ROS scavenging abilities. In the model of rat periodontitis, the PolyLA-GelMA patch inhibits alveolar bone resorption and accelerates the periodontitis healing by regulating the inflammatory microenvironment. This biomacromolecule-stabilized coenzyme polymer patch provides a new option to promote periodontitis treatment.

1. Introduction

Periodontium, including soft tissues (gingiva and periodontal ligament) and hard tissues (cementum and alveolar bone), plays a key role in fixing teeth and transmitting masticatory force [1–3]. Periodontitis is the most common periodontal disease, which is essentially a chronic inflammatory disease caused by pathogenic bacteria. It can lead to alveolar bone resorption and looseness and loss of teeth, seriously reducing the quality of life of patients [4,5]. Periodontal curettage or regenerative periodontal surgery such as bone grafting combined with antibiotic adjuvant therapy is the most commonly method for the treatment of periodontitis in clinical [6–10]. However, due to the complexity and hiding location of periodontal pocket structure and the drug resistance of antibiotics, this traditional treatment cannot achieve effective treatment of periodontitis, and may cause great trauma to patients [11,12]. In addition, due to the high humidity and dynamic characteristics of the oral cavity, it is difficult for antibiotics to be preserved in periodontal lesions, which further reduces the efficiency of treatment. Therefore, it is still urgent to develop an efficient and non-invasive periodontitis treatment strategy.

In recent years, although diverse therapeutic drugs (powders and ointments) have been widely reported to treat periodontitis, they suffer from unsatisfactory treatment efficiency due to their weak adhesion to wet tissue and short retention time (< 1 h) in the highly humid and dynamic environment of the oral cavity [13,14]. To address this limitation, wet tissue adhesives with the three-dimensional network have

Peer review under responsibility of KeAi Communications Co., Ltd.
* Corresponding author.
** Corresponding author.
*** Corresponding author.
E-mail addresses: yzhao@tmu.edu.cn (Y. Zhao), cycui@tju.edu.cn (C. Cui), wgliu@tju.edu.cn (W. Liu).
[1] These authors contributed equally to this work.

https://doi.org/10.1016/j.bioactmat.2024.02.002
Received 26 November 2023; Received in revised form 17 January 2024; Accepted 1 February 2024
2452-199X/© 2024 The Authors. Publishing services by Elsevier B.V. on behalf of KeAi Communications Co. Ltd. This is an open access article under the CC BY-NC-ND license (http://creativecommons.org/licenses/by-nc-nd/4.0/).

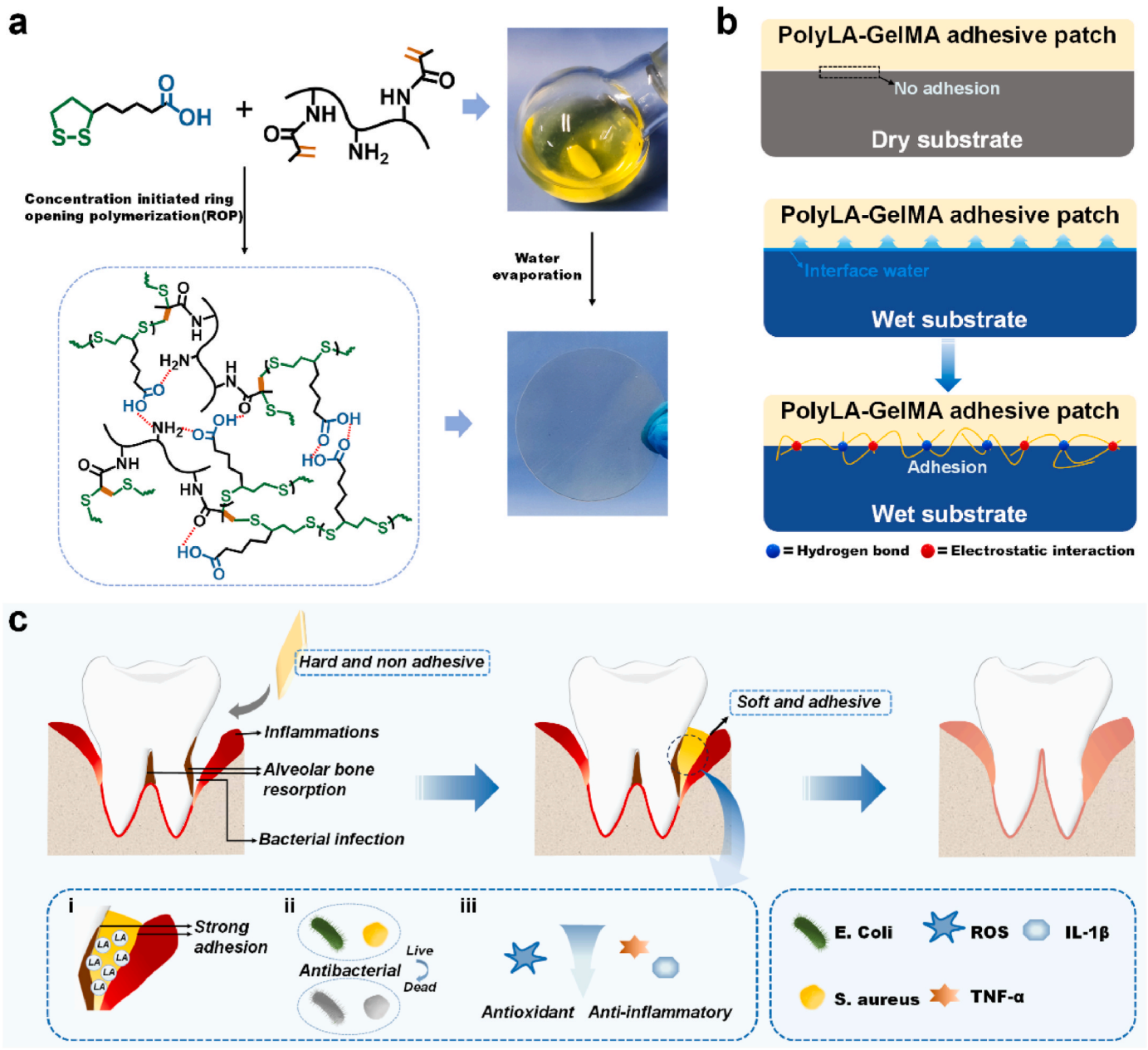

Fig. 1. a) Schematic diagram of preparation process and structural characteristics of PolyLA-GelMA patch. b) Wet-responsive adhesion behavior of PolyLA-GelMA patch. c) Illustration of the proposed mechanism of PolyLA-GelMA patch for promoting periodontitis healing.

been designed and widely used as a platform to allow for the controlled release of therapeutic drugs or cytokines to accelerate the regeneration and remodeling of the periodontal tissue. Among them, injectable adhesive hydrogels for periodontitis treatment have been widely reported because they can be accurately injected into the periodontal pocket [15–17]. However, many injectable adhesive hydrogels require light or heat-assisted gelation, which will greatly increase the complexity of the operation. Besides, when the uncross-linked hydrogel precursor solution is injected into the periodontal pocket, it may spread into the tissue and cause tissue inflammation [18–20]. Adhesive patch can solve these problems of injectable adhesive hydrogels, but it is difficult to insert the adhesive patch into the hidden periodontal pocket because of its weak bulk strength and indiscriminate adhesion to surgical instruments, and many reported adhesive patches often suffer from decreased adhesion or adhesion loss when used in wet and dynamic environment, poor biocompatibility and non-degradability, which will further limit their application in the oral cavity [21–23]. In addition, it is worth noting that most periodontitis treatment materials themselves lack intrinsic therapeutic ability. Although the loading of exogenous drugs, cytokines or proteins can regulate the microenvironment of periodontitis and accelerate periodontal tissue regeneration, this can also increase the cost of treatment or may cause potential drug toxicity [24–26]. Therefore, it is highly desired to develop a self-therapeutic, low-cost, easy insertion delivery and biocompatible bioactive wet tissue adhesive patch to accelerate periodontitis healing.

α-lipoic acid (LA), an endogenous small molecule coenzyme in mitochondria, participates in mitochondrial activity and regulates energy metabolism [27,28]. LA shows excellent antioxidant and anti-inflammation ability based on the disulfide heterocyclic ring in its structure and has been shown to have therapeutic effects in a variety of oxidative stress models, including diabetes, ischemia-reperfusion injury, HIV infection, neurodegeneration and radiation damage [29]. Previous studies also have shown that LA can effectively inhibit periodontal bone loss and kill bacteria by causing the cell membrane dysfunction and

changing in cell morphology [30–32]. In addition, based on the dynamic ring-opening self-polymerization (ROP) properties of sulfur-containing five-membered rings and rich adhesive carboxyl groups, LA has been used to prepare adhesives. However, the as-polymerized poly(α-lipoic acid) (PolyLA) is metastable due to the inverse ring closing depolymerization initiated by terminal reactive radicals [33,34]. Although PolyLA-based polymers can be stabilized by introducing multiple double-bond small molecules or high concentrations of ions, the addition of toxic small molecules and ions significantly reduces the biocompatibility of PolyLA-based polymers [33,35,36]. And the hydrophobicity of PolyLA structure limits the release of LA-based small molecules, which will sacrifice the biological activity of LA. Recently, poly(sodium-lipoate) (PolyLA-Na) has been prepared by simple solvent volatilization, but PolyLA-Na shows water-sensitive dissociation behavior, when it comes into contact with water. In this case, PolyLA-Na is dissociated quickly, but its rapid dissociation rate (<20 min), non-adhesion and rigid nature limit its application in the biomedical field [37].

In this study, aiming at highly efficient treatment of periodontitis, we develop a wet-responsive PolyLA-based elastic patch (PolyLA-GelMA) with water-induced adhesion and softening characteristics by simply concentrating and evaporating a mixed solution of LA, GelMA and tris (hydroxymethyl) aminomethane, in which a small amount of tris (hydroxymethyl) aminomethane is to increase the solubility of LA in water, while GelMA is selected due to its complete natural source and excellent biocompatibility and biodegradability [38–40]. Moreover, the double bonds on the GelMA backbone can quench the sulfur free radicals at the end of PolyLA, thus stabilizing PolyLA (Fig. 1). And the original PolyLA was prepared by concentrating and evaporating a mixed solution of LA and tris (hydroxymethyl) aminomethane without adding GelMA. In the process of solvent evaporation, LA undergoes spontaneous ring-opening polymerization to form PolyLA, while the double bonds on the GelMA can react with the free radicals at the end of PolyLA to prevent PolyLA depolymerization and the multiple hydrogen bonds formed between the amino groups on GelMA and the carboxyl groups on PolyLA further stabilize PolyLA. Moreover, introduction of GelMA polymer chain reduces the layered crystal structure of pristine PolyLA-based polymer, thus decreasing the water-sensitivity of PolyLA-based polymer and prolonging the release time of LA-based active molecules, which is crucial for long-term and effective scavenging of reactive oxygen species (ROS) from the periodontitis microenvironment. A small amount of layered crystal structure retained in the PolyLA-GelMA patch leads to non-adhesiveness and rigidity in a dry environment. Intriguingly, once exposed to water or body fluids, the hydrophilic polymer skeleton of PolyLA-GelMA can quickly absorb water, and the entry of water molecules destroys the layered crystal structure, eventually leading to the generation of soft and adhesive PolyLA-GelMA patch. This wet-responsive PolyLA-GelMA patch has a great advantage in the treatment of periodontitis since the non-adhesion and high hardness in dry state make it easy to insert into the periodontal pocket, which can address the problem of difficult delivery associated with most indiscriminate adhesives. After contact with saliva around the periodontal tissue, the PolyLA-GelMA patch exhibits firm and durable adhesion to tissue quickly by forming multiple hydrogen bonds and electrostatic interactions between the carboxyl groups on PolyLA-GelMA and the amino groups on the tissue surface. In addition, the softness of the PolyLA-GelMA patch after hydration is favorable for filling irregular periodontal defect. Thus, this PolyLA-GelMA patch with wet-triggered adhesion and softening feature is used as a bioactive material in the treatment of periodontitis, and its durable wet-resistant adhesion to tissue can effectively protect the wound from infection, while the continuous release of the LA-based bioactive small molecule can significantly accelerate alveolar bone tissue regeneration by regulating the microenvironment of periodontal injury. In a rat model of ligated periodontitis, the PolyLA-GelMA patch can significantly inhibit alveolar bone resorption. Taken together, this PolyLA-GelMA patch holds a great clinical application prospect in accelerating the repair of periodontitis (Fig. 1).

2. Materials and methods

2.1. Materials

Gelatin (Type A from porcine, 300 g bloom), methacrylic anhydride (97 %) and tris (hydroxymethyl) aminomethane (Tris, 99 %) were purchased from Heowns Biochemical Technologies Co., Ltd. (Tianjin, China). Alpha-lipoic acid (LA, 99 %) was purchased from Macklin (Shanghai, China). Safranine O (85 %), ferrous sulfate heptahydrate ($FeSO_4{\cdot}7H_2O$, 99 %) and hydrogen peroxide (H_2O_2, 30 wt%) were purchased from Aladdin (Shanghai, China). 1,1-Diphenyl-2-picrylhydrazyl free radical (DPPH, 97 %) was purchased from TCI (Shanghai, China). Artificial saliva (99 %) was purchased from Phygene Biotechnology Co., Ltd. (Fuzhou, China). Periocline® (Sunstar, Inc) and Metronidazole Oral Sticking Patches (MAIDI PHARMACY Co., Ltd. Shanxi, China) were used as received. All the other reagents are of analytical grade and used without further purification.

2.2. Synthesize of GelMA

GelMA was synthesized as previously described [41]. Briefly, 4 g of gelatin was dissolved in 200 mL ultrapure water at 40 °C and then 132 mL DMF was added and stirred until the mixed solution became homogeneous and clear. Subsequently, 582 μL methacrylic anhydride was slowly added into the above solution and the reaction proceeded for 2 h at 40 °C. The reaction solution was precipitated in ethanol, and the collected precipitate was then dissolved in deionized water to dialysis and freeze-dried.

2.3. Preparation of PolyLA-GelMA patch

A series of PolyLA-GelMA elastomer patches were obtained through a one-step solvent volatilization concentration method. Briefly, 2 g lipoic acid and 0.8 g tris were dissolved in 15 ml ultrapure water at 65 °C. Then, different proportions of GelMA (0.1 g, 0.2 g, 0.5 g, 1 g, 1.5 g) were added into the above solution and stirred for 2 h at 65 °C. Subsequently, the mixture solution was poured into the mold and PolyLA-GelMA-x patch could be obtained after the aqueous solution evaporated completely. The preparation of original PolyLA patch was consistent with the above steps except without adding GelMA.

2.4. Characterizations

The chemical structures of gelatin and GelMA were characterized by ^{1}H NMR spectra on a nuclear magnetic resonance (NMR) spectrometer (AVANCE III, 400 MHz, Bruker) using D_2O as the solvent. The methacylation degree of GelMA was defined as in previous report [42].

The polymerization process of LA was recorded by a UV spectrophotometer (GENESYS 180, Thermo Fisher Scientific). First, the UV spectrum of the mixed solution was tested using a pure GelMA solution as a control. Subsequently, the mixed solution was poured into a quartz substrate and dried completely to obtain PolyLA-GelMA elastomeric films as test sample. ^{1}H NMR spectra of LA, PolyLA and PolyLA-GelMA were determined in DMSO-d6, DMSO-d6 and D_2O respectively on a nuclear magnetic resonance (NMR) spectrometer (AVANCE IIITM HD 400 MHZ Nano BAY, Bruker). Raman spectra were recorded on a Renishaw laser Raman spectrometer (inVia reflex) excited at 532 nm. Attenuated total reflection (ATR) infrared spectra were recorded by a Fourier transform infrared (FTIR) spectrometer (Nicolet IS10, Thermo-Fisher Scientific). The spectral range was 400–4000 cm^{-1}. The crystal structures of PolyLA and PolyLA-GelMA-x were determined on an X-ray diffractometer (XRD) (D8 Advanced, Bruker, Germany). XRD data were obtained from 3 to 50° (2θ) using Cu Kα radiation at a scan rate of 1°

min^{-1}. The contact angles were measured at room temperature on an optical contact goniometer (Harke-SPCA, China) after 5 μL of deionized water was dropped on the elastomer surface. Herein, each sample was photographed and recorded at the 20th second. The average value of contact angle was calculated from at least 3 times measurements for each sample using Image J software (NIH USA, 2008). The dynamic temperature scanning of the PolyLA-GelMA-25 was tested before and after being placed in 90 % RH for 3 h with a strain of 0.1 % and a frequency of 1 Hz.

2.5. Mechanical properties of PolyLA-GelMA patch

The mechanical properties of PolyLA-GelMA-x elastomers at room temperature were tested using the Instron 2344 micro testing machine in an air environment. At least three samples were tested for each characterization. During the tensile test, all samples were cut into a size of 30 mm × 5 mm, and the tensile speed was set to 50 mm/min [43]. In order to simulate the characteristics of elastomers in humid environments, the PolyLA-GelMA-x elastomer sheets (30 mm × 5 mm) were placed in a 90 % RH for 30 min and 3 h respectively before testing.

To evaluate the self-healing ability of the patch in humid environment at 37 °C, inverted fluorescence microscopy was used to take photos of the scratch film before and after self-healing at different time points.

2.6. Adhesion properties of PolyLA-GelMA patch

The Instron 2344 Micro tester was used to test the adhesion properties of PolyLA-GelMA-x. Lap-shear testing was performed to measure the adhesive strength of the PolyLA-GelMA-x to different substrates. The PolyLA-GelMA patch was applied to the surface of pig skin tissue, oral mucosa, stomach, large intestine, small intestine, and heart with a bonding area of 10 mm × 10 mm at 37 °C. Before adhering to glass, the PolyLA-GelMA patch was placed in a 90 % RH for 10 min and applied to the surface of glass with a bonding area of 10 mm × 10 mm. After adhesion, the two ends of the substrates were clamped, respectively. Then, the substrates were pulled upwards at a constant speed of 50 mm/min, while the F was recorded. The adhesion strength was calculated as F/WL, where F is the maximum load force during lap shear stretching, and W and L are the width and length of the rectangular patch, respectively. All the tests were repeated three times.

T peeling test: PolyLA-GelMA-x elastomer patches were adhered to the porcine skin from the same end at 37 °C, and the adhesion width (w) was recorded. The other two ends of the tissues were clamped separately and pulled upward at a speed of 50 mm/min and the force F was recorded. The interfacial toughness of the elastomer adhesive to the tissue was calculated as 2F/w.

2.7. In vitro release of LA-based monomer

The release of LA-based monomer from PolyLA-GelMA-x elastomer patches in vitro was studied by incubating the sample (2 mg/ml) in artificial saliva at 37 °C. The absorbance of the supernatant at a wavelength of 330 nm was measured by Ultraviolet spectrophotometer (GENESYS 180 Thermo Fisher Scientific) at different time points [44]. The release amount of LA-based small molecular monomer was calculated by standard curve equation.

2.8. Antioxidant activity

The scavenging ability of PolyLA-GelMA-x on DPPH was carried out in accordance with previous reports [45]. Briefly, 10 mg PolyLA-GelMA-x was mixed with 1 mL DPPH solution (0.05 mmol/L, 80 wt% methanol) for 12 h. The absorbance of the supernatant at 517 nm wavelength was measured by a UV spectrophotometer (GENESYS 180, Thermo Fisher Scientific). The control group was the pure DPPH solution under an identical condition. The DPPH scavenging ability of PolyLA-GelMA-x was calculated using the following formula: DPPH scavenging ability (%) = (AC − AS)/AC × 100 %, where AC and AS are the absorbance of the control and sample group.

The scavenging ability of PolyLA-GelMA-x on hydroxyl radicals was evaluated by Fenton reaction [45]. Briefly, 600 μL $FeSO_4$ solution (2 mmol/L), 500 μL safranin O solution (360 μg/mL) and 10 mg samples were mixed first and incubated for 10 min. Subsequently, 800 μL of H_2O_2 (6 wt%) solution was added to the above solution and incubated at 55 °C for 30 min. 300 μL ultrapure water was used to replace sample as the blank group and 1100 μL ultrapure water was used to replace sample and H_2O_2 as the control group. At the scheduled time, the solution was cooled down to room temperature and the absorbance of the supernatant at 492 nm was examined on a microplate reader (Infnite M200 PRO, Tecan, Switzerland). The ·OH scavenging ability was calculated using the following formula: ·OH scavenging ability (%) = (AS - AB)/(AC -AB) × 100 %, where AS, AC and AB are the absorbance of the sample, control and blank group.

The scavenging ability of PolyLA-GelMA-x on ABTS radicals was tested by following the instructions of the ABTS free radical scavenging efficiency kit (Beyotime). All tests were repeated three times.

2.9. In vitro antibacterial capability of PolyLA-GelMA

1 ml bacterial suspension of Escherichia coli (E. coli) or Staphylococcus aureus (S. aureus) (10^5 CFU mL^{-1}) was mixed with 20 mg PolyLA-GelMA-x and cultured at 37 °C for 12 and 24 h. The untreated bacterial suspension was set as control group. The values of different groups in OD600 were recorded and the bacterial survival rate was calculated by the value of OD600. For agar plate test, the bacterial suspension cultured with PolyLA-GelMA-x for 12 h was uniformly coated on an agar plate and allowed to incubate for 8 h at 37 °C, and the colony growth was recorded by taking photos. Moreover, the bacterial morphology of the blank group and PolyLA-GelMA-25 patch group was observed by scanning electron microscope.

2.10. Hemolysis assay

The rate of hemolysis of PolyLA-GelMA-x elastomer was tested according to previous methods [46].

2.11. Live/dead assay

Live/Dead assay was used to verify the biocompatibility of the PolyLA-GelMA-x. Periodontal ligament stem cells (PDLSCs) were evenly spread in 48-well plates. After the cells were attached, 200 μL of α-MEM complete medium containing different concentrations of PolyLA-GelMA (5 μg/ml and 10 μg/ml) was added to each well, followed by Live/Dead staining experiment, and incubated at 37 °C for 30 min in the dark. Under the fluorescence microscope, the living cells were stained green under the action of Calcein-AM, and the dead cells were infiltrated by PI and emitted red fluorescence.

2.12. Cytotoxicity assay

CCK-8 method was used to detect the effect of different concentrations of PolyLA-GelMA-x treatment on the proliferation of PDLSCs. The well-growing PDLSCs were taken out, digested and centrifuged. After that, the cells were counted under the microscope, and spread evenly on the 96-well plate at a density of 5000 cells/well. After the cells were attached, 100 μL of α-MEM complete medium containing different concentrations of PolyLA-GelMA (5 μg/ml and 10 μg/ml) was added to each well and cultured at 37 °C. At the 24th and 72nd h of culture, 10 μL CCK-8 solution was added to each well, and the absorbance at 450 nm was measured by a microplate reader after 2 h of culture at 37 °C.

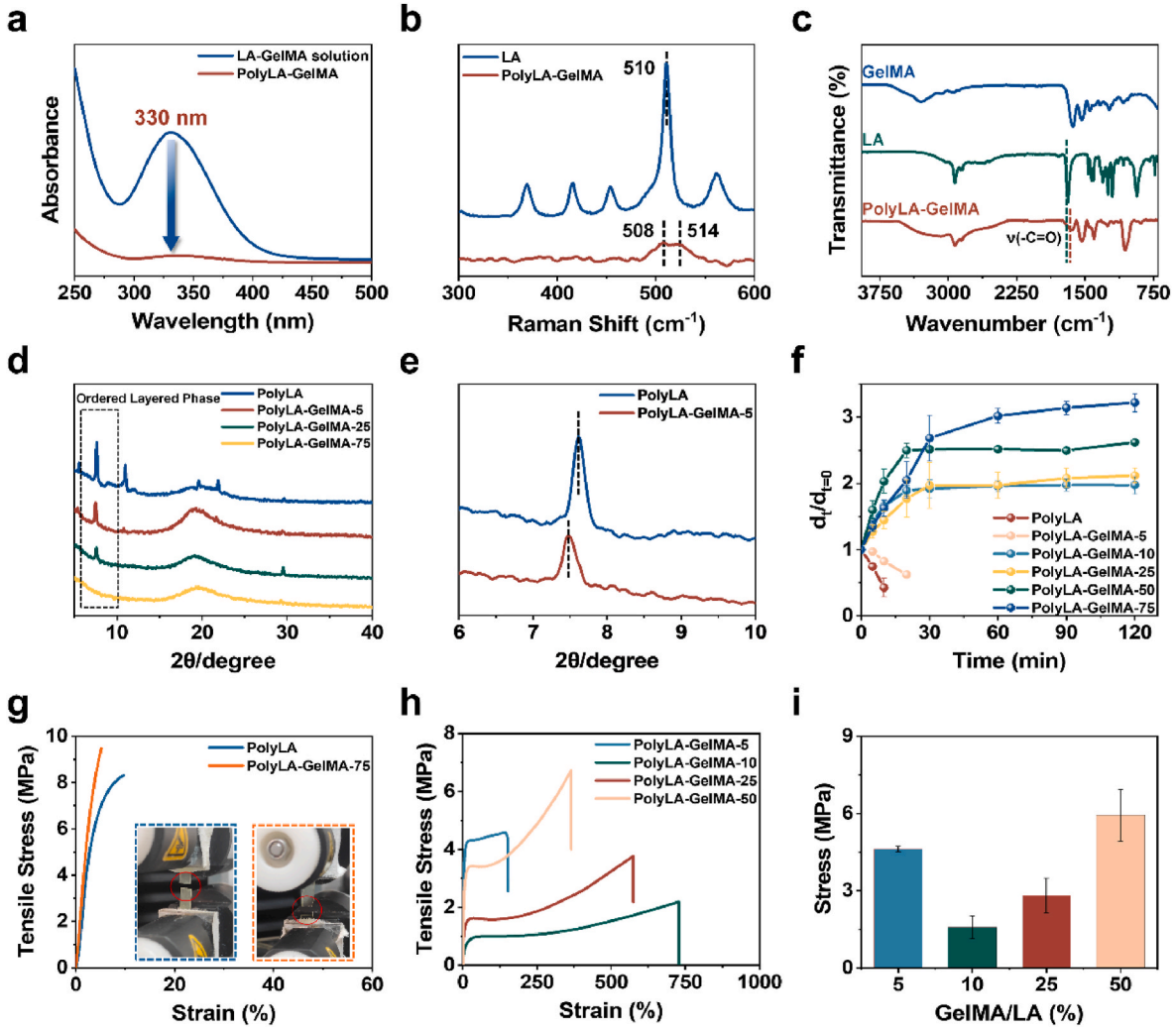

Fig. 2. a) UV–vis absorption spectra of LA-GelMA solution and dry PolyLA-GelMA patch; b) Raman spectra of the LA powder, and PolyLA-GelMA-25; c) ATR-IR spectra of the LA, PolyLA-GelMA-25 and GelMA; d) XRD patterns of PolyLA and PolyLA-GelMA-x; e) XRD patterns of PolyLA and PolyLA-GelMA-5; f) Diameter change of PolyLA-GelMA patches after immersing in water at 37 °C for different time; g) Tensile curves and tensile images of PolyLA and PolyLA-GelMA-75; h) Tensile curves of PolyLA-GelMA with different GelMA content; i) Tensile stress of PolyLA-GelMA with different GelMA content (n = 3).

2.13. In vitro cell antioxidant evaluation

The cell oxidative stress model was established, and the ability of PolyLA-GelMA-x to scavenge ROS in cell was verified. First, DCFH-DA was diluted with serum-free culture medium at a final concentration of 10 μM according to 1: 1000 and PDLSCs were seeded in 48-well plates and treated with 200 μM H_2O_2 for 6 h to establish a cell oxidative stress model. Next, the H_2O_2 was removed, and 200 μL of α-MEM complete medium containing PolyLA-GelMA-x (5 μg/ml) was added to each well. Finally, the cell culture medium was removed and the appropriate volume of diluted DCFH-DA was added. After that, the cells were incubated at 37 °C for 20 min. The cells were washed three times with serum-free cell culture medium to fully remove the free DCFH-DA and observed under a fluorescence microscope. Similarly, after staining, the cells were digested with trypsin, washed three times with PBS, and the levels of ROS were detected using flow cytometry (LSRFortessa, BD, America).

2.14. Animal experiments

All the animal experiments were complied with the guidelines of the Tianjin Medical Experimental Animal Care, and animal protocols were approved by the Institutional Animal Care and Use Committee of Yi Shengyuan Gene Technology (Tianjin) Co., Ltd. (protocol number YSY-DWLL-2023235). SD rats weighing approximately 230 g were used in this study. Immediately before surgery, the rats were anesthetized using pentobarbital sodium. First of all, the rat model of periodontitis was made. The oral cavity of rats was opened, and 0.25 mm orthodontic ligature wire was ligated to the bilateral maxillary second molars of rats. After modeling, the mental state and eating status of rats in each group were observed, and the ligature wire was checked regularly. After 4 weeks, the ligation wire was removed and the gelatin, PolyLA-GelMA-25, Metronidazole Oral Sticking Patches (MTZ) and Periocline® (PERIO) were placed in the buccal and palatal gingival sulcus and replaced once a week for four weeks. After the treatment, the rats were euthanized, and the maxillary bone was resected and fixed in 4 % paraformaldehyde for 24 h. After the fixation was completed, the maxillary bone was rinsed with water and PBS, and the alveolar bone resorption was analyzed by micro-CT. CT Vox software and Data Viewer software were used to reconstruct the three-dimensional digital image and tomographic image of the alveolar bone, and the distance between the alveolar ridge (ABC) and the cementoenamel junction (CEJ) was measured. The bone mineral density (BMD), bone volume (BV), tissue volume (TV) and its ratio (BV/TV) around the ligated molars were further calculated by CTAn software. The analysis area we selected for BMD and BV/TV was the alveolar bone around the maxillary second molar. After that, H&E, Masson and immunohistochemical staining

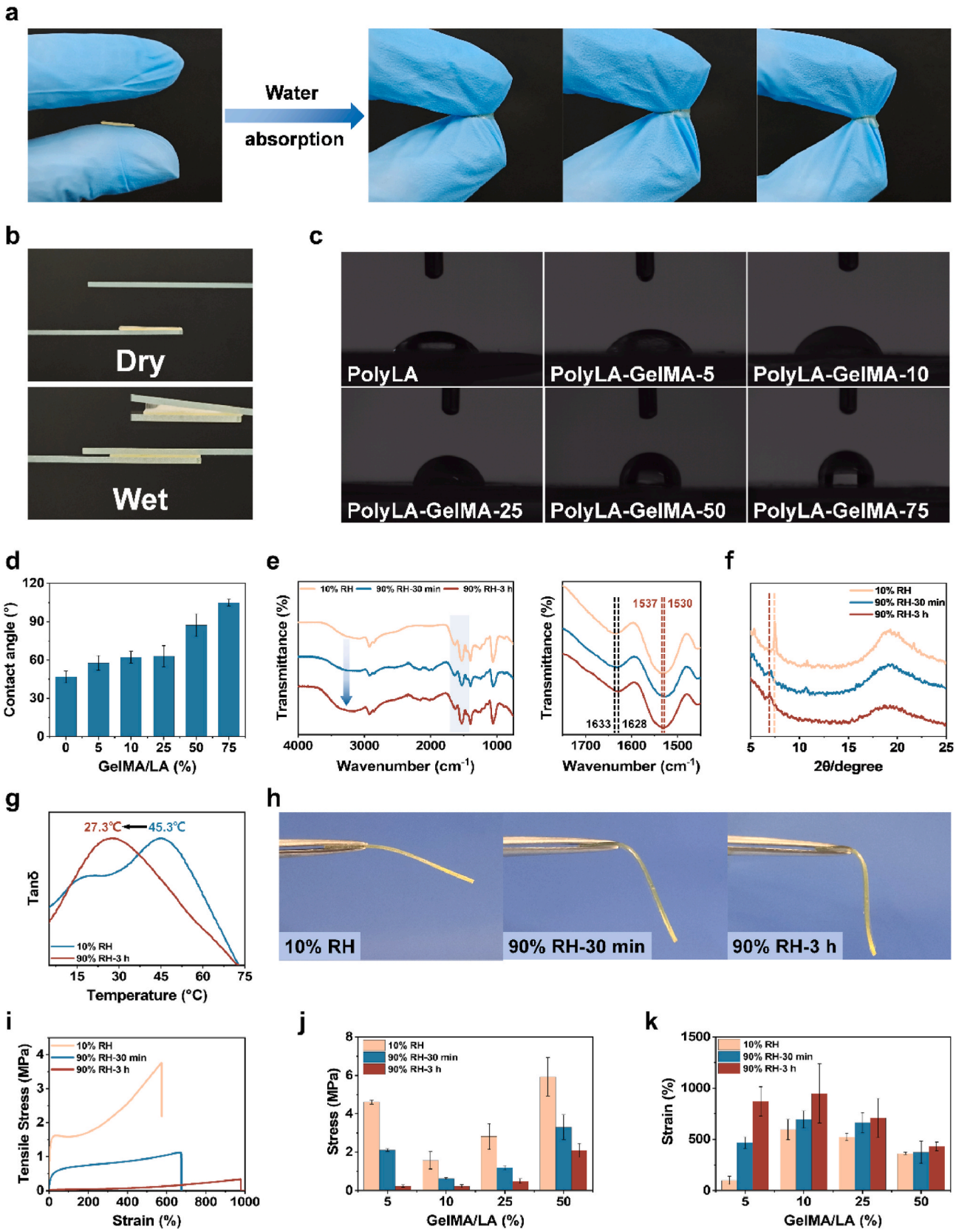

Fig. 3. a) Wet-responsive adhesion behavior of PolyLA-GelMA-25; b) Image of PolyLA-GelMA-25 adhesion to glass before and after placement in 90 % RH environment for 10 min; c, d) Water contact angle of original PolyLA and PolyLA-GelMA-x (n = 3); e) ATR-IR spectra of PolyLA-GelMA-25 in different states; f) XRD patterns of PolyLA-GelMA-5 in different states; g) DMA curves of PolyLA-GelMA-25 in different states; h) Macroscopic state of PolyLA-GelMA-25 in different states; i) Tensile curves of PolyLA-GelMA-25 at different conditions; j) Tensile stress of PolyLA-GelMA-x in different states (n = 3); k) Tensile strain of PolyLA-GelMA-x in different states (n = 3).

were performed on the maxillary tissue.

2.15. Statistical analysis

All results were expressed as mean ± standard deviation (SD) and statistical analysis was performed by one-way analysis of variance (ANOVA). Statistical differences were defined as *$p < 0.05$, **$p < 0.01$, ***$p < 0.001$ and ****$p < 0.0001$.

3. Results and discussion

3.1. Preparation and characterization of PolyLA-GelMA patch

In this study, PolyLA-GelMA patches were prepared simply by mixing LA with GelMA in different mass ratios in aqueous solution and then evaporating the water completely without further treatment. GelMA was used as a crosslinking agent to quench the sulfur free radicals at the end of PolyLA and thus prevent PolyLA depolymerization (Fig. 1a). The obtained PolyLA-GelMA patch was named as PolyLA-GelMA-x, where x represented the mass percentage of GelMA to LA. The successful preparation of GelMA was verified through ^{1}H NMR spectra. As shown in Fig. S1, the characteristic peaks of vinyl methacrylate appeared at 5.4 and 5.7 ppm, indicating the successful preparation of GelMA. The methacylation degree of GelMA was determined to be 72 % [41]. The spontaneous ring opening and polymerization characteristics of LA with solvent evaporation was recorded by UV–vis spectra. As shown in Fig. 2a, the absorption peak of the disulfide-containing five-membered ring in LA monomer at 330 nm in the LA-GelMA solution disappeared after the PolyLA-GelMA patch was formed by solvent volatilization, suggesting that LA indeed underwent ring-opening polymerization spontaneously during the concentration process [44]. ^{1}H NMR spectra proved the efficient copolymerization reaction of LA and GelMA (Fig. S2) [47]. The successful ROP of LA in PolyLA-GelMA could also be confirmed from the splitting of the characteristic Raman peak at 510 cm^{-1} for disulfide bonds in the five-membered ring into two peaks at 509 and 514 cm^{-1} wavenumbers [48], which once again verified that PolyLA was stable in PolyLA-GelMA (Fig. 2b). The interaction between PolyLA and GelMA in PolyLA-GelMA patch was further confirmed by the attenuated total reflection infrared (ATR-IR) spectra (Fig. 2c), the –C═O peak on the carboxylate in the PolyLA-GelMA patch exhibited an obvious red shift compared to the pristine LA monomer, implying that strong hydrogen bond interaction between ─COOH in LA and $–NH_2$ in GelMA occurred [27]. X-ray diffraction (XRD) was used to illustrate the structural changes of PolyLA-GelMA in different proportions. As shown in Fig. 2d, sharp diffraction peaks in the small angle region (less than 20°) appeared in original PolyLA, indicating that there was a highly ordered nanoscale crystal structure in PolyLA. This was due to the hierarchical self-assembly of LA during the solvent evaporation self-polymerization process [37]. With the addition of GelMA, the diffraction peak intensity of PolyLA in the small angle region gradually decreased and eventually disappeared, indicating the transformation of PolyLA-GelMA patches with different GelMA content from crystal structure to amorphous structure. Comparing the XRD results of the PolyLA and PolyLA-GelMA-5 revealed that the diffraction angle of PolyLA decreased after mixing with GelMA (Fig. 2e), indicating that the addition of GelMA increased the interlayer distance of PolyLA and reduced the crystallinity of PolyLA (Table S1). At higher contents of GelMA, the layered crystal structure of PolyLA could be destroyed completely.

As described above, the PolyLA is highly water sensitive and it dissociates quickly in water, which will limit its application in the biomedical field [37]. After the introduction of GelMA into PolyLA, multiple covalent and hydrogen bond crosslinking significantly reduced its water sensitivity and slowed down its dissociation rate in water. As shown in Fig. 2f, after contact with water, original PolyLA dissociated completely within 20 min, and the dissociation rate of PolyLA-GelMA-x patches with different GelMA content decreased obviously. When the GelMA content was 10 % and above, PolyLA-GelMA remained stable and did not dissociate in water. The mechanical properties of PolyLA and PolyLA-GelMA-x patches were evaluated by tensile test. The ordered layered crystal structure in the PolyLA makes it too brittle to be stretched (Fig. 2g) [37]. For PolyLA-GelMA-x patch, with the increase of GelMA content, the tensile strength decreased at first and then increased, while the elongation increased at first and then decreased. (Fig. 2h and i and Fig. S3). This is because the addition of GelMA reduced the layered ordered crystal structure of the original PolyLA, thus resulting in a decrease in the tensile strength and increase in the elongation of PolyLA-GelMA. However, when the content of GelMA was high, the multiple covalent and hydrogen bonding interaction between PolyLA and GelMA increased the cross-linking density of PolyLA-GelMA network, thereby enhancing the tensile strength again and reducing the elongation of PolyLA-GelMA. When the GelMA content continued to increase to 75 %, brittle fracture occurred when tensile test was carried out (Fig. 2g). Therefore, the mechanical properties of PolyLA-GelMA patches could be adjusted by changing the content of GelMA.

3.2. Wet-responsive behavior of PolyLA-GelMA patch

The adhesion performance of PolyLA-GelMA patch was studied next. Take PolyLA-GelMA-25 as an example, we found that the patch was not adhesive in the dry state since its ordered layered structure limited the movement of polymer chains and surface adhesion groups. However, it gained adhesion ability after being placed at 90 % relative humidity (90 % RH) for 10 min (Fig. 3a and b and Video S1). This is because the hydrophilic dry PolyLA-GelMA patch could quickly absorb the water in the wet environment, and the water molecules could be used as a plasticizer to break the layered orderly arrangement between the polymer chains [49], which increased the mobility of the polymer chain and surface adhesion groups, thus resulting in interface adhesion of patch. The adhesion strength of PolyLA-GelMA patches with different GelMA contents to glass was tested after 10 min of placement at 90 % RH. As shown in Fig. S4, with the increase of GelMA content, the adhesion strength of PolyLA-GelMA to glass increased at first and then decreased, and when the content of GelMA was 25 %, the adhesion strength was the highest and could reach 127.0 kPa. A possible reason was that when the GelMA content was less than 25 %, the introduction of GelMA could increase the cross-linking density of the polymer network, thus enhancing the bulk strength of the patch, which was very important for efficient adhesion. If the GelMA content was further increased above 25 %, too dense cross-linking in the polymer network limited the adsorption and transport of water molecules, which affected the movement of polymer chains, thereby resulting in the decrease of adhesion strength. Therefore, the PolyLA-GelMA patch showed wet-responsive adhesion behavior, which was suitable for effective administration in the treatment of periodontitis. In order to verify our conjecture, we first tested the water contact angle of different components of PolyLA-GelMA patches. As shown in Fig. 3c and d, the original PolyLA exhibited the smallest contact angle due to its high hydrophilicity and ordered layered crystal structure [37]. With the addition of GelMA, the water contact angle of PolyLA-GelMA increased, and when the content of GelMA was more than 25 %, the water contact angle increased significantly, indicating that the introduction of GelMA destroyed the layered structure of the polymer network and increased the cross-linking density, thus reducing the adsorption of water, which was consistent with our previous discussion. The wet-responsive mechanism of PolyLA-GelMA was investigated by ATR-IR spectroscopy (Fig. 3e). The peak intensity of –OH on the carboxyl in PolyLA-GelMA increased gradually around 3400 cm^{-1}, suggesting the presence of bound water in the polymer network after the patch was placed in 90 % RH for different time. And the slight red shift of carboxylic acid groups in PolyLA from 1633 to 1628 cm^{-1} and amino groups in GelMA from 1537 to 1530 cm^{-1} respectively after absorbing water was observed, indicating that the hydration of

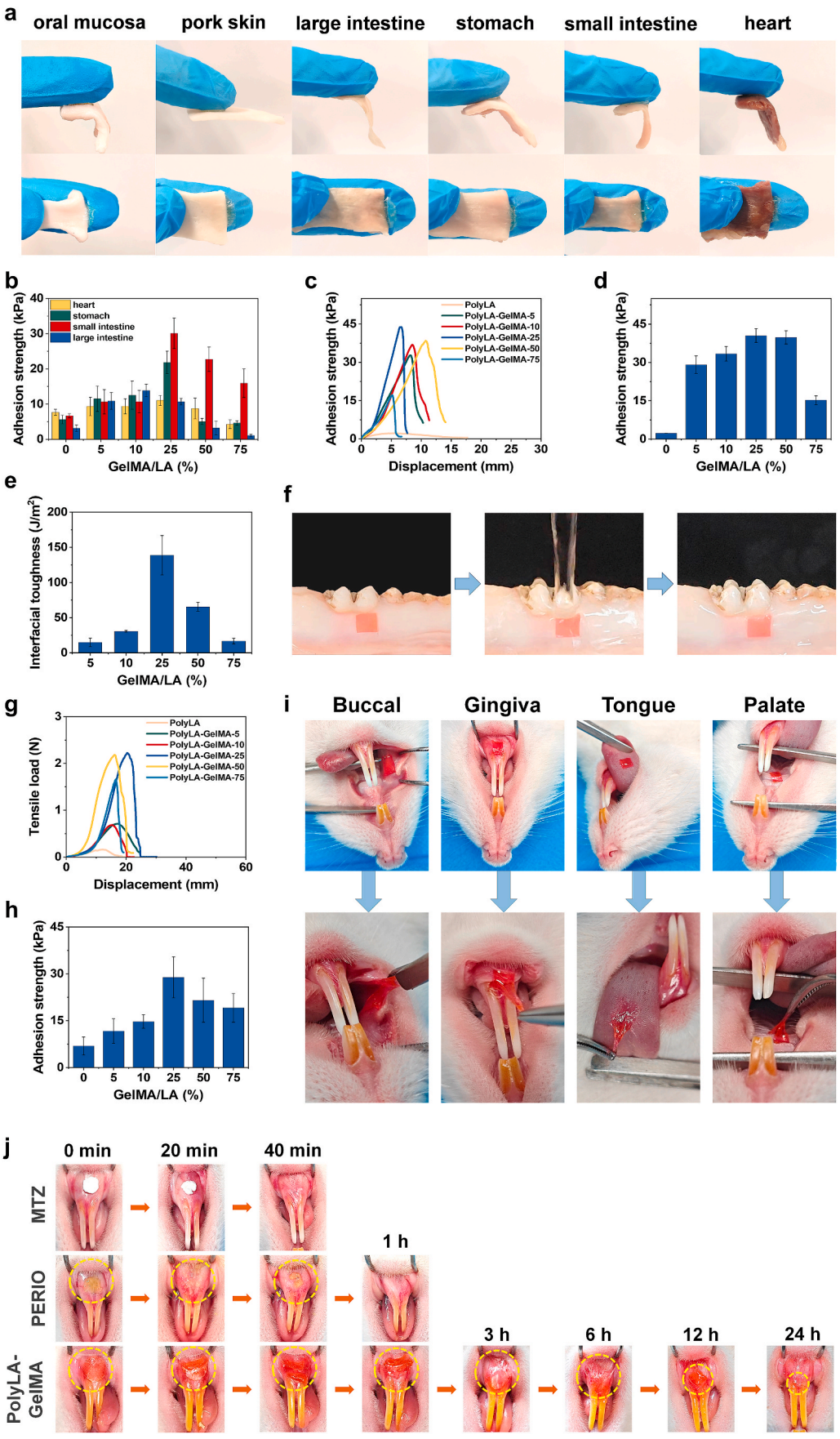

(caption on next page)

Fig. 4. a, b) Adhesion ability and adhesion strength of PolyLA-GelMA-25 patch to various wet tissues; c, d) Lap shear curves (c) and adhesion strength (d) of PolyLA-GelMA-x patches to pig skin (n = 3); e) Interfacial toughness of PolyLA-GelMA-x to pig skin (n = 3); f) Photographs showing that the PolyLA-GelMA-25 patch could tightly adhere to the gingiva tissue of pig under a violent water-flushing condition; g, h) Lap shear curves (g) and adhesion strength (h) of PolyLA-GelMA-x patches to oral mucosa (n = 3); i) Photographs showing that the PolyLA-GelMA-25 patch could tightly adhere to different parts of the rat oral cavity and withstand stretch movement; j) Durable adhesion ability of PolyLA-GelMA-25, MTZ and PERIO in oral cavity.

carboxylic acid groups and amino groups occurred [37,49]. XRD tests were performed to characterize the crystal structural changes of PolyLA-GelMA before and after water absorption. As shown in Fig. 3f, the diffraction angle of PolyLA-GelMA decreased with increasing water absorption time, indicating interlayer distance increased after adsorbing water molecules [27]. When PolyLA-GelMA was immersed in water, the diffraction peak of the crystalline phase of PolyLA-GelMA disappeared completely, hinting that the PolyLA-GelMA was highly hydrated and amorphous phase was dominant (Fig. S5). Therefore, PolyLA-GelMA could become softened after adsorbing water. The results of dynamic mechanical analysis showed that the ordered layered crystal structure of the PolyLA-GelMA network in the dry state led to a high glass transition temperature (Tg = 45.3 °C) (Fig. 3g), suggesting that the segmental movement was not sufficient to form adhesion interactions with the substrates; therefore, PolyLA-GelMA showed no adhesion in the dry state. However, upon water absorption, the glass transition temperature of PolyLA-GelMA decreased to 27.3 °C since the water molecules destroyed the layered crystal structure of PolyLA-GelMA and the polymer chains were high flexible, allowing sufficient interaction of the carboxylate groups with the substrates to achieve adhesion.

The self-healing property of PolyLA-GelMA also proved the fast motility of the polymer chain after being placed in 90 % RH for 6 h (Fig. S6). The mechanical properties of PolyLA-GelMA after absorbing water were also investigated. Consistent with the above discussion, the PolyLA-GelMA patches with different compositions were softened obviously after being placed in 90 % RH for different time (Fig. 3h). Their tensile stress decreased and the elongation increased compared with dried PolyLA-GelMA (Fig. 3i–k). The wet-responsive softness feature of PolyLA-GelMA is beneficial for oral applications, which increases the comfort of patients.

3.3. Tissue adhesion behavior of PolyLA-GelMA patch

The oral cavity is a highly wet and dynamic environment, so designing an adhesive patch with a lasting and firm adhesion ability in the oral cavity is very important for the treatment of periodontitis [13]. As mentioned above, the PolyLA-GelMA patch was wet-responsive and could absorb water quickly in a wet environment, which allowed it to quickly remove the interfacial hydration layer when used in oral cavity. Therefore, when it came into contact with wet oral tissue, the patch could eliminate the hydration layer on the tissue interface quickly and achieve close adhesion with the tissue by forming multiple hydrogen bonds or electrostatic interactions. As shown in Fig. 4a, PolyLA-GelMA could securely adhere to various wet tissues, including oral mucosa, pig skin, large intestine, stomach, small intestine and myocardial tissue. And the adhesion strength of PolyLA-GelMA-x to various wet tissues was tested (Fig. 4b). The adhesion strength of PolyLA-GelMA-x patches to wet pig skin was tested at 37 °C. As shown in Fig. 4c–e and Fig. S7, the original PolyLA patch had the lowest adhesion strength due to its rapid dissociation when it came into contact with wet tissue. However, the adhesion strength of PolyLA-GelMA patch increased at first and then decreased with the increment of GelMA content, and when the GelMA content was 25 %, the adhesion strength and the interface toughness reached the maximum of 40.5 kPa and 138.8 J/m^2. The adhered pig skin could easily lift 100 g weight without falling. The reason was that the introduction of GelMA increased the cross-linking density of the polymer network, which in turn enhanced the wet stability and cohesion strength of the patch. When the content of GelMA was 25 %, the interface energy and cohesion energy of the patch reached a balance, so it showed the best adhesion performance. When the content of GelMA was less than 25 %, the interface energy of the patch was greater than the cohesion energy, so it exhibited cohesion failure in the adhesion strength test. Whereas when the content of GelMA was higher than 25 %, the cohesion energy of the patch was greater than the interface energy; in this case, the patch showed interface failure (Fig. S7). In addition, when the content of GelMA was high, the dense cross-linking network limited water absorption, which was unfavorable for removing the hydration layer on the interface of wet tissue, affecting the wet adhesion of the patch.

Next, the adhesion ability of PolyLA-GelMA patches to oral tissue was also examined. As shown in Fig. 4f, Video S2 and Video S3, PolyLA-GelMA patch adhered immediately to the wet gingival tissue of pig once in contact, and could withstand a violent water flushing without the occurrence of peeling-off, indicating strong adhesion of the PolyLA-GelMA patch to the oral tissue. The adhesion strength of PolyLA-GelMA patches to porcine oral mucosa was measured by lap-shear test. Consistent with the above results, the PolyLA-GelMA-25 showed the highest adhesion strength to oral mucosa, which was up to 28.9 kPa (Fig. 4g and h). In addition, we found that the epithelium on the surface of oral mucosa could be peeled off when PolyLA-GelMA-25 was used for oral mucosa peel test, which once again proved the excellent adhesion of PolyLA-GelMA-25 to oral mucosa (Fig. S8).

Supplementary video related to this article can be found at https://doi.org/10.1016/j.bioactmat.2024.02.002

The oral cavity is a humid and dynamic environment, and the lasting adhesion of the patch in the oral cavity is essential for drug retention and continuous delivery. As shown in Fig. 4i, the PolyLA-GelMA-25 could achieve firm adhesion to the wet tissue surface of the rat buccal, gingiva, tongue and palate. Tweezers were used to stretch PolyLA-GelMA-25 patch to simulate oral movement. Obviously, the PolyLA-GelMA-25 patch could still adhere to the tissue without falling off, demonstrating its secure wet and dynamic tissue adhesion. In addition, the durable adhesion of the PolyLA-GelMA patch to gingival tissue was also tracked and compared with the commercial periodontitis drugs (Metronidazole oral sticking patches (MTZ) and Perio minocycline hydrochloride ointment (PERIO)). Remarkably, our PolyLA-GelMA patch could firmly adhere to the oral mucosa for about 24 h, while the MTZ and PERIO were dissolved within 1 h (Fig. 4j). Moreover, compared with MTZ and PERIO, the PolyLA-GelMA patch could adhere to oral tissue more tightly, which was more beneficial to the treatment of periodontitis. The indiscriminate adhesion of traditional adhesive patches makes them difficult to be inserted into the periodontal pocket. In this work, the wet responsive adhesion behavior of PolyLA-GelMA patch can circumvent drawback of traditional soft adhesives. These results suggest that PolyLA-GelMA patch is promising to be a patch for oral periodontitis repair.

3.4. Biocompatibility, antioxidation and antibacterial activity of PolyLA-GelMA patch

Many studies have confirmed that LA has excellent antioxidant activities [50,51]. LA has been shown to alleviate the irreversible damage of tooth support tissue caused by excessive ROS in periodontitis model [30]. However, the intrinsic hydrophobicity of the PolyLA hinders the entry of water into the polymer network, so it is difficult to release LA-based bioactive small molecule during application [52]. The conventional method is combination with other drugs to achieve ideal antioxidant effect [53]. The PolyLA-GelMA patches obtained in this

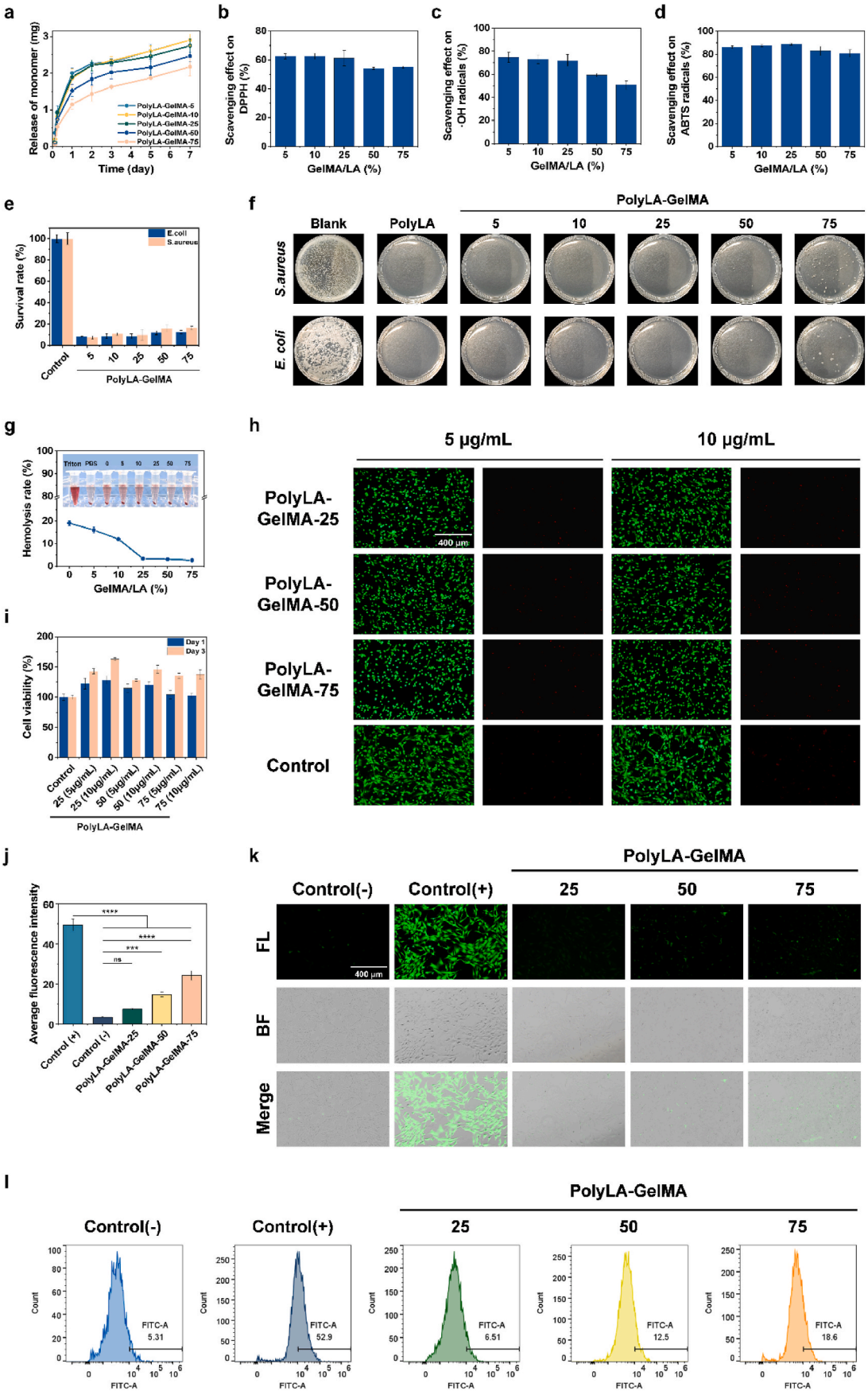

(caption on next page)

Fig. 5. a) Monomer release amount of PolyLA-GelMA-x patches in artificial saliva; b-d) Scavenging efficiency of PolyLA-GelMA-x on DPPH radicals (b), hydroxyl radicals (c), and ABTS radicals (d); e) Survival rates of E. coli and S. aureus after co-incubating with PolyLA-GelMA-x patches for 12 h; f) Digital images displaying colony growth of *S. aureus* and *E. coli* on agar plates after co-culture with PolyLA-GelMA-x; g) Hemolysis rate of PolyLA-GelMA-x patches; h) Live/dead staining of PDLSCs co-cultured with PolyLA-GelMA-x patches for 24 h; i) Cell viability of PDLSCs co-cultured with PolyLA-GelMA-x patches for 1 and 3 days; j, k) Average fluorescence intensity (j) and fluorescence microphotographs (k) of the DCFH-DA ROS detection assay on PDLSCs treated with PolyLA-GelMA-x patches for 24 h; l) Flow cytometry analysis of cells labeled with DCFH-DA in FITC-A channels on different patches. Data are expressed as mean ± SD. The significant difference was detected by one-way ANOVA. n = 3, ***p < 0.001, and ****p < 0.0001.

work by solvent volatilization concentrated polymerization had a hydrophilic skeleton, which was beneficial to the release of LA-based bioactive small molecules without loading external drug. Therefore, the LA-based bioactive monomer release behavior of PolyLA-GelMA patches in artificial saliva was evaluated. As shown in Fig. 5a and Fig. S9, all the adhesive patches could sustainably release the LA-based monomer during the 7-day testing process, and the release efficiency of all patches could reach about 50 %. This means that the introduction of GelMA suppressed the rapid dissociation of PolyLA network and avoided the explosive release of LA-based monomers. Moreover, the long-term release of LA-based active molecules was conducive to the continuous regulation of periodontal inflammatory microenvironment. Next, the antioxidation effect of PolyLA-GelMA patches on 1,1-diphenyl-2-picryl-hydrazyl free radical (DPPH), hydroxyl radicals (·OH) and ABTS radicals was tested to characterize their ROS scavenging activity. As shown in Fig. 5b, the PolyLA-GelMA patches could achieve about 60 % DPPH scavenging efficiency after 12 h. Fig. S10 shows that the purple color of the DPPH solution turned yellow after 12 h of incubation with PolyLA-GelMA patches, indicating that the patches could efficiently scavenge DPPH radicals. Then the Fenton reaction was used to determine the inhibitory effect of PolyLA-GelMA patches on ·OH (Fig. 5c). The PolyLA-GelMA-5, PolyLA-GelMA-10 and PolyLA-GelMA-25 were shown to achieve 70 % ·OH scavenging efficiency after 30 min incubation, but the scavenging efficiency of PolyLA-GelMA-50 and PolyLA-GelMA-75 to ·OH decreased slightly. This is attributed to the less amounts of LA-based monomers released by PolyLA-GelMA-50 and PolyLA-GelMA-75 than other patches. A similar trend was also manifested in the clearance of ABTS radicals (Fig. 5d). The scavenging ability of PolyLA-GelMA-5, PolyLA-GelMA-10 and PolyLA-GelMA-25 on ABTS radicals was higher than 86 %, and the scavenging ability of PolyLA-GelMA-50 and PolyLA-GelMA-75 could also reach 82 % and 80 %, respectively. The scavenging ability of PolyLA-GelMA patches on various free radicals was related to the effective release of LA-based bioactive small molecule, demonstrating its excellent antioxidant activity. The warm and humid oral environment makes the oral cavity a breeding ground for various bacteria, which can cause serious infection to the periodontitis wound. Therefore, effective antibacterial is also the key to the treatment of periodontitis [54]. For PolyLA-GelMA patch, the released LA-based monomer could kill both Gram-positive bacteria and Gram-negative bacteria by depolarizing the bacterial cell membrane and increasing the permeability of the bacterial cell membrane [32,55]. As shown in Fig. 5e and Fig. S11, the survival rates of both E. coli and S. aureus showed a significant decrease (less than 20 %) after 12 and 24 h of co-culture with PolyLA-GelMA patch. Furthermore, it can be seen from Fig. 5f that the growth of bacterial colonies was significantly inhibited after co-cultured with PolyLA-GelMA-x patch. Moreover, compared with the blank group, the surface membrane structure of bacteria co-cultured with PolyLA-GelMA shrank seriously (Fig. S11). All these results indicated that the PolyLA-GelMA patch had a high antibacterial efficiency. An ideal tissue adhesive should induce no or little hemolysis upon contacting bleeding damaged tissue. Thus, in vitro hemolysis test was used to evaluate the blood compatibility of the PolyLA-GelMA patches. The illustration in Fig. 5g showed photographs of the whole blood centrifuge supernatant treated with Triton X-100 positive group, phosphate buffered saline (PBS) negative group, and PolyLA-GelMA-x groups. The PolyLA-GelMA-25, 50 and 75 groups were all transparent bright yellow, similar to the PBS negative group, while the PolyLA, PolyLA-GelMA-5 and PolyLA-GelMA-10 groups were light red. Moreover, the hemolysis rate of PolyLA-GelMA patches decreased with the increase of GelMA content. When the GelMA content was less than 25 %, the hemolysis rate was higher than 5 %, and when the GelMA content was further increased, the hemolysis rate decreased to less than 5 %. The reason is that when the content of GelMA was low, the rapid release of LA monomer led to increased hemolysis. Therefore, the PolyLA-GelMA-25, PolyLA-GelMA-50 and PolyLA-GelMA-75 with good blood compatibility were selected for subsequent cell experiments.

The cytotoxicity of PolyLA-GelMA patches was first determined using live/dead staining by coculturing periodontal ligament stem cells (PDLSCs) with different mass of PolyLA-GelMA patches. As shown in Fig. 5h, the PDLSCs spread evenly and survived, which was indicated by observing rich green fluorescent spots in the fluorescent image obtained by live/dead assay. Quantitative analysis of live/dead staining shows that the cell viability after co-culturing with PolyLA-GelMA-25, PolyLA-GelMA-50 and PolyLA-GelMA-75 were all higher than 97.5 %, indicating that PolyLA-GelMA patches had good cytocompatibility (Fig. S12). Then CCK-8 test was performed to verify the ability of PolyLA-GelMA-25, PolyLA-GelMA-50 and PolyLA-GelMA-75 to promote the proliferation of PDLSCs. As shown in Fig. 5i, 10 μg/mL concentration of PolyLA-GelMA-x promoted cell proliferation obviously after co-culturing for 3 days. Moreover, PolyLA-GelMA-25 had the highest cell proliferation rate, followed by PolyLA-GelMA-50 and PolyLA-GelMA-75. These results suggested that LA was an effective bioactive molecule for promoting cell proliferation.

2′, 7′-Dichlorofluorescin diacetate (DCFH-DA) assay fluorescent probe is an oxidation-sensitive test used as a general marker of intracellular ROS [56]. We next used DCFH-DA to determine the antioxidant activity of PolyLA-GelMA patches (5 μg/mL) on PDLSCs. The results of the DCFH-DA assay showed that the decrease in fluorescence intensity was proportional to the released LA-based monomer content of the PolyLA-GelMA patches, and the fluorescence intensity of PolyLA-GelMA-25, PolyLA-GelMA-50 and PolyLA-GelMA-75 decreased by 85 %, 70 % and 51 %, respectively (Fig. 5j and k). The decrease in fluorescence represented an increase in antioxidant activity, confirming the ability of the released LA-based monomer from patch to protect PDLSCs from oxidative stress. In addition, flow cytometry (Fig. 5l) results showed that the ROS positivity rates of PolyLA-GelMA-25, 50, and 75 decreased to 6.5 %, 12.5 %, and 18.6 %, respectively. These results indicated that the PolyLA-GelMA adhesive patch exhibited a strong antioxidation effect, among which PolyLA-GelMA-25 had the best antioxidant activity. Therefore, considering the satisfactory wet adhesion performance, suitable mechanical property, good cell compatibility and antioxidant ability, we chose PolyLA-GelMA-25 for the treatment of periodontitis in rats in the following study.

3.5. Therapeutic effects of periodontitis in the rat model

Prior to the therapeutic study, in vivo degradation and histocompatibility of PolyLA-GelMA-25 were assessed through subcutaneous implantation experiments. The PolyLA-GelMA-25 completely degraded after subcutaneous implantation for 7 days. The H&E staining results showed that compared with the normal tissue, there was no significant inflammation in the subcutaneous tissue after treated with the PolyLA-GelMA-25 patch for 7 days (Fig. S13). Histological assessment of major organs including the heart, liver, spleen, lung, and kidney revealed that the PolyLA-GelMA-25 patch did not cause any damage to these organs (Fig. S13). These data proved that PolyLA-GelMA-25 patch

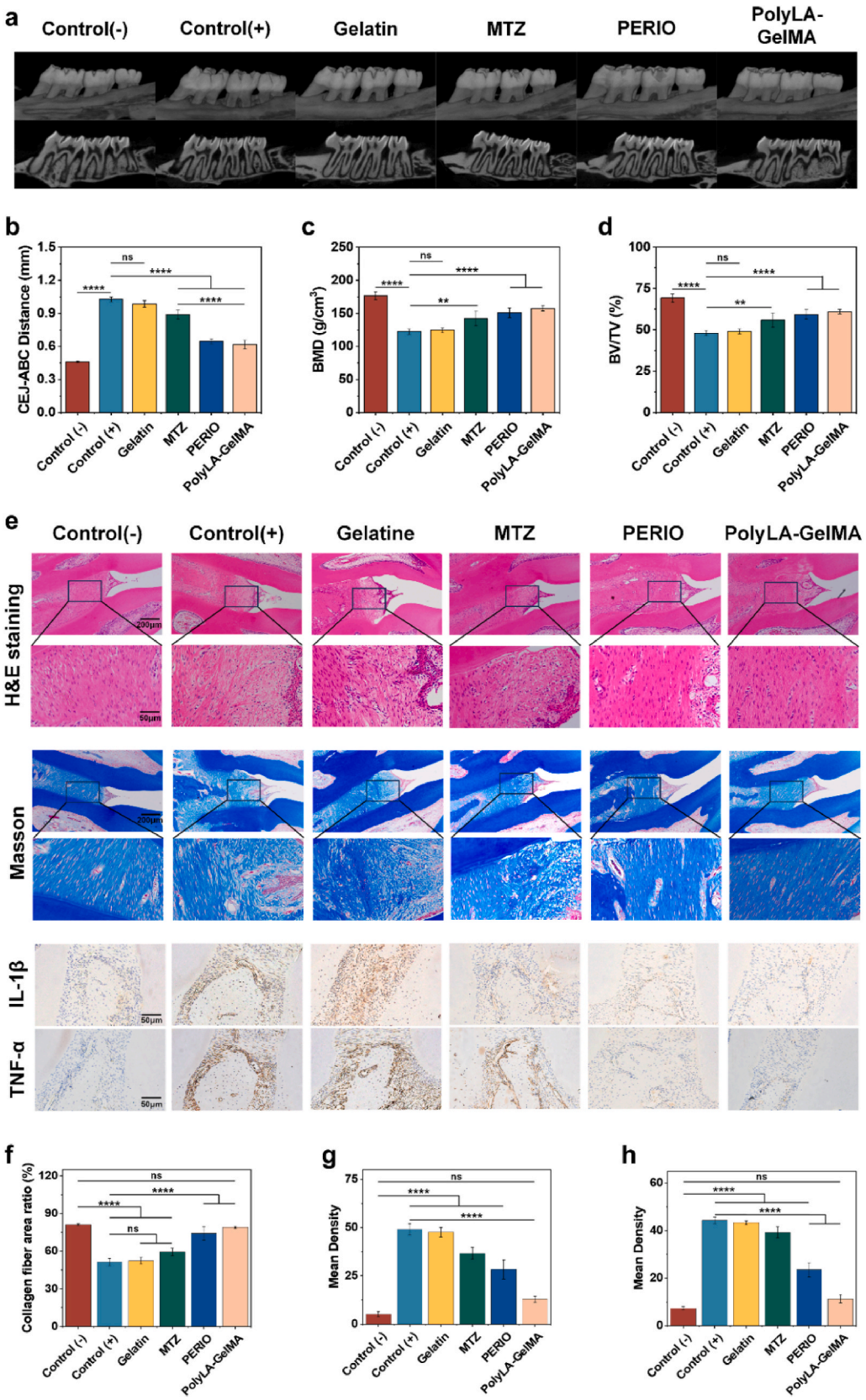

Fig. 6. a) 3D reconstruction micro-CT and 2D images of the maxillary alveolar bone of the 4th week after treatment; b-d) Quantification of CEJ-ABC distance (b), BMD (c), and BV/TV (d); e) H&E staining, Masson staining and immunohistochemistry staining of TNF-α and IL-1β antibodies of the repaired periodontal tissue at 28 days; f) Quantification of the collagen fiber area ratio of gingival tissues after treated with different groups through Masson staining; g, h) Quantitative analysis of expression levels TNF-α (g) and IL-1β (h) antibodies in restored periodontal tissues after 28 days of repair. Data are means ± SD. The significant difference was detected by one-way ANOVA. n = 5, *p < 0.05, **p < 0.01, ***p < 0.001, and ****p < 0.0001.

did not bring about local or systemic toxicity to rats, showing good biosafety and biocompatibility. In order to verify the therapeutic effect of the PolyLA-GelMA patch on periodontitis, we used PolyLA-GelMA-25 patch, pure gelatin patch and commercial PERIO and MTZ as treatment groups; normal rats served as negative control group (control (−)) and the untreated group as a positive control group (control (+)). Compared with commercial materials, PolyLA-GelMA-25 was easier to insert into periodontal pocket because of its hardness nature in dry state. The patch was softened quickly and adhered closely to periodontal tissue after adsorbing saliva and gingival crevicular fluid.

Alveolar bone resorption was analyzed by using micro-computed tomography (micro-CT) after repairing for 28 days. 3D reconstructed images and tomographic images of the alveolar bone were reconstructed using CT Vox software and Data Viewer software, respectively. As shown in Fig. 6a, compared with control (−) group, control (+) group showed significant alveolar bone resorption, confirming the successful construction of the periodontitis model. After treatment, the degree of alveolar bone resorption in the Gelatin group was similar to that in the control (+) group, indicating that gelatin alone had no therapeutic effect on periodontitis. Although MTZ, PERIO, and PolyLA-GelMA patch all showed inhibition of alveolar bone resorption, PolyLA-GelMA patch group exhibited the best inhibitory effect. To further evaluate the restoration of alveolar bone, the CEJ-ABC distance, bone mineral density (BMD), and bone volume fraction (BV/TV) of each group were measured. The results showed that compared with the control (+) group, the CEJ-ABC distance of the other groups was smaller (Fig. 6b), but there was no significant difference in the CEJ-ABC distance between the Gelatin group and the control (+) group, once again confirming that Gelatin had no therapeutic effect on periodontitis. Compared with the control (+) group and the Gelatin group, the CEJ-ABC distance of the MTZ, PERIO and PolyLA-GelMA groups all showed a declined trend. In comparison, the PolyLA-GelMA group was the closest to the control (−) group. Similarly, the BMD and BV/TV of the PolyLA-GelMA group were the highest compared with other groups, which proved that the release of LA-based bioactive molecules of PolyLA-GelMA patch could effectively alleviate alveolar bone resorption in periodontitis model (Fig. 6c and d).

H&E and Masson staining were performed to evaluate the periodontium healing of different treatment groups at the histological level. As shown in Fig. 6e and f, there were obvious degeneration and degradation of elastic and collagen fibers caused by inflammation in control (+), Gelatin and MTZ groups, indicating that the periodontal tissue was seriously damaged in these three groups. We speculated that the poor therapeutic effect of MTZ may be attributed to its short residence time on the surface of periodontal tissue. However, the PolyLA-GelMA patch and PERIO groups achieved good therapeutic effects on periodontal tissue repair, showing thicker epithelial cell layers, less infiltration of inflammatory cells, denser elastic and collagen fiber tissues, and more regular arrangement.

Next, immunohistochemistry staining for the expression of inflammatory cytokines of interleukin-1β (IL-1β) and tumor necrosis factor-α (TNF-α) around periodontal microenvironment were evaluated (Fig. 6e). As shown in Fig. 6g and h, both the control (+) and Gelatin groups exhibited a high expression of IL-1β and TNF-α antibody in the periodontal tissue of rats, indicating that gelatin alone had no anti-inflammatory effect. There was a slight decrease in the levels of IL-1β and TNF-α antibody expression in the MTZ group. In contrast, there was a significant decrease in the expression of the two inflammatory factors in the groups of PolyLA-GelMA and PERIO, close to the control (−) group. This was consistent with the results of micro-CT and histological staining, implying that PolyLA-GelMA was effective in relieving periodontal inflammation and promoting alveolar bone repair. The tissue compatibility of PolyLA-GelMA in the oral cavity was also evaluated by H&E staining at the end of the 4 weeks of treatment. H&E staining of major organs including heart, liver, spleen, lungs and kidney revealed that the PolyLA-GelMA-25 adhesive patch did not cause any damage and inflammation to these organs (Fig. S14). These data proved that PolyLA-GelMA-25 had long-term biosafety when used in vivo. All these results supported that the PolyLA-GelMA-25 adhesive patch has great potential in the treatment of periodontitis, and its therapeutic effect is comparable to that of the most common PERIO ointment in the market.

4. Conclusions

In this work, we fabricated methacrylated gelatin (GelMA)-stabilized co-enzyme polymer poly(α-lipoic acid) (PolyLA)-based elastic patch with water-triggered adhesion and softening characteristics. Different from the intrinsic hydrophobicity of PolyLA, the PolyLA-GelMA was hydrophilic, so it could achieve the continuous release of LA-based bioactive small molecules when used in wet environment. The previously reported PolyLA patch prepared by solvent volatilization concentration method showed a strong water sensitivity, and PolyLA could dissociate quickly in water, while incorporation of GelMA significantly increased the wet stability of the patch, and prolonged the dissociation rate of the PolyLA-GelMA patch in water from 20 min to about 24 h by forming multiple covalent and hydrogen bonding crosslinks between the GelMA and the PolyLA. Interestingly, the PolyLA-GelMA patch was non-sticky and hard in the dry state, which was favorable for the insertion of patch into the periodontal cavity in comparison with traditional adhesives. Once exposed to water, its hydrophilic skeleton absorbed water quickly, resulting in softening and adhesion, which could improve the comfort of the patient, and aided in fixing on the wound site and continuously delivering LA-based bioactive molecules. In vitro studies revealed that the PolyLA-GelMA patch possessed satisfactory antibacterial, blood compatibility and ROS scavenging abilities. Moreover, subcutaneous implantation experiments demonstrated that the PolyLA-GelMA patch could be completely degraded within 7 days and showed good biological safety. Upon applying PolyLA-GelMA patch onto the periodontitis tissue of rats, long-lasting adhesion to wound tissue and water-triggered the sustainable release of LA-based bioactive small molecules from the patch played an anti-inflammatory and antioxidant role in regulating the microenvironment of the periodontitis wound, thus considerably inhibiting alveolar bone resorption and alleviating inflammatory reactions. We anticipate that this study will provide an approach to develop other wet tissue adhesives in the future for periodontitis treatment.

Ethics approval and consent to participate

All the animal experiments were complied with the guidelines of the Tianjin Medical Experimental Animal Care, and animal protocols were approved by the Institutional Animal Care and Use Committee of Yi Shengyuan Gene Technology (Tianjin) Co., Ltd. (protocol number YSY-DWLL-2023235).

CRediT authorship contribution statement

Ying Qi: Writing – original draft, Methodology, Investigation, Formal analysis, Data curation. **Chenyu Xu:** Investigation, Formal analysis, Data curation. **Zhuodan Zhang:** Investigation, Data curation. **Qian Zhang:** Investigation, Data curation. **Ziyang Xu:** Software, Data curation. **Xinrui Zhao:** Investigation, Data curation. **Yanhong Zhao:** Formal analysis, Conceptualization. **Chunyan Cui:** Writing – original draft, Formal analysis, Conceptualization. **Wenguang Liu:** Writing – review & editing, Formal analysis, Conceptualization.

Declaration of competing interest

The authors declare no conflicts of interest.

Acknowledgements

The authors gratefully acknowledge the support for this work from the National Natural Science Foundation of China (Grant No. 52233008, 52303201).

Appendix A. Supplementary data

Supplementary data to this article can be found online at https://doi.org/10.1016/j.bioactmat.2024.02.002.

References

[1] M. Cho, P. Garant, Development and general structure of the periodontium, Periodontol 24 (2000) 9–27, 2000.
[2] A. Tomokiyo, N. Wada, H. Maeda, Periodontal ligament stem cells: regenerative potency in periodontium, Stem Cell. Dev. 28 (2019) 974–985.
[3] J. Gong, C. Ye, J. Ran, X. Xiong, X. Fang, X. Zhou, Y. Yi, X. Lu, J. Wang, C. Xie, J. Liu, Polydopamine-mediated immunomodulatory patch for diabetic periodontal tissue regeneration assisted by metformin-ZIF system, ACS Nano 17 (2023) 16573–16586.
[4] L. Wu, S. Zhang, L. Zhao, Z. Ren, C. Hu, Global, regional, and national burden of periodontitis from 1990 to 2019: results from the Global Burden of Disease study 2019, J. Periodontol. 93 (2022) 1445–1454.
[5] E. Kononen, M. Gursoy, U. Gursoy, Periodontitis: a multifaceted disease of tooth-supporting tissues, J. Clin. Med. 8 (2019) 1135.
[6] S. Zegaib, J. Lage-Marques, M. Vieira, A. Junior, M. Feres, J. Shibli, L. Figueiredo, Phenomenon of laser power loss during curettage of infected periodontal pockets, Photomed. Laser Surg. 29 (2011) 657–662.
[7] R. Chace, Subgingival curettage in periodontal therapy, J. Periodontol. 45 (1974) 107–109.
[8] M. Bottino, V. Thomas, G. Schmidt, Y. Vohra, T. Chu, M. Kowolik, G. Janowski, Recent advances in the development of GTR/GBR membranes for periodontal regeneration-a materials perspective, Dent. Mater. 28 (2012) 703–721.
[9] L. Nibali, J. Buti, L. Barbato, F. Cairo, F. Graziani, S. Jepsen, Adjunctive effect of systemic antibiotics in regenerative/reconstructive periodontal surgery-A Systematic Review with Meta-Analysis, Antibiotics 11 (2021) 8.
[10] C. Chu, X. Zhao, S. Rung, W. Xiao, L. Liu, Y. Qu, Y. Man, Application of biomaterials in periodontal tissue repair and reconstruction in the presence of inflammation under periodontitis through the foreign body response: recent progress and perspectives, J. Biomed. Mater. Res., Part B 110 (2021) 7–17.
[11] J. Slots, M. Ting, Systemic antibiotics in the treatment of periodontal disease, Periodontol 28 (2000) 106–176, 2002.
[12] M. Umeda, Y. Takeuchi, K. Noguchi, Y. Huang, G. Koshy, I. Ishikawa, Effects of nonsurgical periodontal therapy on the microbiota, Periodontol 36 (2004) 98–120, 2000.
[13] M. Huang, Y. Huang, H. Liu, Z. Tang, Y. Chen, Z. Huang, S. Xu, J. Du, B. Jia, Hydrogels for the treatment of oral and maxillofacial diseases: current research, challenges, and future directions, Biomater. Sci. 10 (2022) 6413–6446.
[14] W. Zhang, B. Bao, F. Jiang, Y. Zhang, R. Zhou, Y. Lu, S. Lin, Q. Lin, X. Jiang, L. Zhu, Promoting oral mucosal wound healing with a hydrogel adhesive based on a phototriggered S-Nitrosylation coupling reaction, Adv. Mater. 33 (2021) 2105667.
[15] S. Hu, L. Wang, J. Li, D. Li, H. Zeng, T. Chen, L. Li, X. Xiang, Catechol-modified and MnO_2-nanozyme-reinforced hydrogel with improved antioxidant and antibacterial capacity for periodontitis treatment, ACS Biomater. Sci. Eng. 9 (2023) 5332–5346.
[16] Z. Dong, Y. Sun, Y. Chen, Y. Liu, C. Tang, X. Qu, Injectable adhesive hydrogel through a microcapsule cross-link for periodontitis treatment, ACS Appl. Bio Mater. 2 (2019) 5985–5994.
[17] X. Zhao, Y. Yang, J. Yu, R. Ding, D. Pei, Y. Zhang, G. He, Y. Cheng, A. Li, Injectable hydrogels with high drug loading through B-N coordination and ROS-triggered drug release for efficient treatment of chronic periodontitis in diabetic rats, Biomaterials 282 (2022) 121387.
[18] Z. Hu, Y. Zhou, H. Wu, G. Hong, M. Chen, W. Jin, W. Lu, M. Zuo, Z. Xie, J. Shi, An injectable photopolymerizable chitosan hydrogel doped anti-inflammatory peptide for long-lasting periodontal pocket delivery and periodontitis therapy, Int. J. Biol. Macromol. 252 (2023) 126060.
[19] Y. Liu, T. Li, M. Sun, Z. Cheng, W. Jia, K. Jiao, S. Wang, K. Jiang, Y. Yang, Z. Dai, L. Liu, G. Liu, Y. Luo, ZIF-8 modified multifunctional injectable photopolymerizable GelMA hydrogel for the treatment of periodontitis, Acta Biomater. 146 (2022) 37–48.
[20] Z. Shen, S. Kuang, Y. Zhang, M. Yang, W. Qin, X. Shi, Z. Lin, Chitosan hydrogel incorporated with dental pulp stem cell-derived exosomes alleviates periodontitis in mice via a macrophage-dependent mechanism, Bioact. Mater. 5 (2020) 1113–1126.
[21] J. Yu, Y. Qin, Y. Yang, X. Zhao, Z. Zhang, Q. Zhang, Y. Su, Y. Zhang, Y. Cheng, Robust hydrogel adhesives for emergency rescue and gastric perforation repair, Bioact. Mater. 19 (2023) 703–716.
[22] H. An, Z. Gu, L. Zhou, S. Liu, C. Li, M. Zhang, Y. Xu, P. Zhang, Y. Wen, Janus mucosal dressing with a tough and adhesive hydrogel based on synergistic effects of gelatin, polydopamine, and nano-clay, Acta Biomater. 149 (2022) 126–138.
[23] Y. Zhang, C. Cui, Y. Sun, X. Zhang, R. Yang, J. Yang, F. Xie, W. Liu, A hyperbranched polymer-based water-resistant adhesive: durable underwater adhesion and primer for anchoring anti-fouling hydrogel coating, Sci. China Technol. Sci. 65 (2021) 201–213.
[24] Z. Gan, Z. Xiao, Z. Zhang, Y. Li, C. Liu, X. Chen, Y. Liu, D. Wu, C. Liu, X. Shuai, Y. Cao, Stiffness-tuned and ROS-sensitive hydrogel incorporating complement C5a receptor antagonist modulates antibacterial activity of macrophages for periodontitis treatment, Bioact. Mater. 25 (2023) 347–359.
[25] B. Wang, J. Wang, J. Shao, P. Kouwer, E. Bronkhorst, J. Jansen, X. Walboomers, F. Yang, A tunable and injectable local drug delivery system for personalized periodontal application, J. Contr. Release 324 (2020) 134–145.
[26] X. Zhang, M. Hasani-Sadrabadi, J. Zarubova, E. Dashtimighadam, R. Haghniaz, A. Khademhosseini, M. Butte, A. Moshaverinia, T. Aghaloo, S. Li, Immunomodulatory microneedle patch for periodontal tissue regeneration, Matter 5 (2022) 666–682.
[27] C. Cui, Y. Sun, X. Nie, X. Yang, F. Wang, W. Liu, A coenzyme-based deep eutectic supramolecular polymer bioadhesive, Adv. Funct. Mater. (2023) 2307543.
[28] C. Liu, R. Lu, M. Jia, X. Xiao, Y. Chen, P. Li, S. Zhang, Biological glue from only lipoic acid for scarless wound healing by anti-inflammation and TGF-β regulation, Chem. Mater. 35 (2023) 2588–2599.
[29] B. Salehi, Y. Berkay Yılmaz, G. Antika, T. Boyunegmez Tumer, M. Fawzi Mahomoodally, D. Lobine, M. Akram, M. Riaz, E. Capanoglu, F. Sharopov, N. Martins, W. Cho, J. Sharifi-Rad, Insights on the use of α-lipoic acid for therapeutic purposes, Biomolecules 9 (2019) 365.
[30] L. Wang, Y. Li, M. Ren, X. Wang, L. Li, F. Liu, Y. Lan, S. Yang, J. Song, pH and lipase-responsive nanocarrier-mediated dual drug delivery system to treat periodontitis in diabetic rats, Bioact. Mater. 18 (2022) 254–266.
[31] K. Tsuji-Naito, Additive inhibitory effects of alpha-lipoic acid with cinnamaldehyde against osteoclastogenesis, Food Sci. Technol. Res. 16 (2010) 353–358.
[32] C. Shi, Y. Sun, X. Zhang, Z. Zheng, M. Yang, H. Ben, K. Song, Y. Cao, Y. Chen, X. Liu, R. Dong, X. Xia, Antimicrobial effect of lipoic acid against Cronobacter sakazakii, Food Control 59 (2016) 352–358.
[33] Q. Zhang, C. Shi, D. Qu, Y. Long, B. Feringa, H. Tian, Exploring a naturally tailored small molecule for stretchable, self-healing, and adhesive supramolecular polymers, Sci. Adv. 4 (2018) 8.
[34] Y. Wang, S. Sun, P. Wu, Adaptive ionogel paint from room-temperature autonomous polymerization of α-thioctic acid for stretchable and healable electronics, Adv. Funct. Mater. 31 (2021) 2101494.
[35] W. Zheng, Y. Li, H. Wei, G. Gao, D. Zhang, Z. Jiang, Rapidly self-healing, magnetically controllable, stretchable, smart, moldable nanoparticle composite gel, New J. Chem. 44 (2020) 10586–10591.
[36] X. Ke, S. Tang, Z. Dong, K. Ren, P. Yu, X. Xu, J. Yang, J. Luo, J. Li, An instant, repeatable and universal supramolecular adhesive based on natural small molecules for dry/wet environments, Chem. Eng. J. 442 (2022) 136206.
[37] Q. Zhang, Y. Deng, H. Luo, C. Shi, G. Geise, B. Feringa, H. Tian, D. Qu, Assembling a natural small molecule into a supramolecular network with high structural order and dynamic functions, J. Am. Chem. Soc. 141 (2019) 12804–12814.
[38] Y. Cui, S. Hong, Y. Xia, X. Li, X. He, X. Hu, Y. Li, X. Wang, K. Lin, L. Mao, Melatonin engineering M2 macrophage-derived exosomes mediate endoplasmic reticulum stress and immune reprogramming for periodontitis therapy, Adv. Sci. 10 (2023) 2302029.
[39] L. Roldan, C. Montoya, V. Solanki, K. Cai, M. Yang, S. Correa, S. Orrego, A Novel injectable piezoelectric hydrogel for periodontal disease treatment, ACS Appl. Mater. Interfaces 15 (2023) 43441–43454.
[40] N. Li, L. Xie, Y. Wu, Y. Wu, Y. Liu, Y. Gao, J. Yang, X. Zhang, L. Jiang, Dexamethasone-loaded zeolitic imidazolate frameworks nanocomposite hydrogel with antibacterial and anti-inflammatory effects for periodontitis treatment, Mater. Today Bio 16 (2022) 100360.
[41] B. He, J. Wang, M. Xie, M. Xu, Y. Zhang, H. Hao, X. Xing, W. Lu, Q. Han, W. Liu, 3D printed biomimetic epithelium/stroma bilayer hydrogel implant for corneal regeneration, Bioact. Mater. 17 (2022) 234–247.
[42] X. Zhao, X. Nie, X. Zhang, Y. Sun, R. Yang, X. Bian, Q. Zhang, H. Wang, Z. Xu, W. Liu, 3D printed β-sheet-reinforced natural polymer hydrogel bilayer tissue engineering scaffold, Sci. China Technol. Sci. 66 (2023), https://doi.org/10.1007/s11431-023-2471-0.
[43] M. Xiao, Y. Yao, W. Liu, Durable and stretchable nanocomposite ionogels with high thermoelectric property for low-grade heat harvesting, Sci. China Technol. Sci. 66 (2022) 267–280.
[44] Q. Zhang, Y. Deng, C.-Y. Shi, B.L. Feringa, H. Tian, D.-H. Qu, Dual closed-loop chemical recycling of synthetic polymers by intrinsically reconfigurable poly (disulfides), Matter 4 (2021) 1352–1364.
[45] Y. Liu, R. Guo, T. Wu, Y. Lyu, M. Xiao, B. He, G. Fan, J. Yang, W. Liu, One zwitterionic injectable hydrogel with ion conductivity enables efficient restoration of cardiac function after myocardial infarction, Chem. Eng. J. 418 (2021) 129352.
[46] X. Bian, C. Cui, Y. Qi, Y. Sun, Z. Zhang, W. Liu, Amino acid surfactant-induced superfast gelation of silk fibroin for treating noncompressible hemorrhage, Adv. Funct. Mater. 32 (2022) 2207349.
[47] C. Shi, Q. Zhang, B. Wang, M. Chen, D. Qu, Intrinsically photopolymerizable dynamic polymers derived from a natural small molecule, ACS Appl. Mater. Interfaces 13 (2021) 44860–44867.
[48] C. Cui, B. Liu, T. Wu, Y. Liu, C. Fan, Z. Xu, Y. Yao, W. Liu, A hyperbranched polymer elastomer-based pressure sensitive adhesive, J. Mater. Chem. A 10 (2022) 1257–1269.
[49] C. Shi, Q. Zhang, B. Wang, D. He, H. Tian, D. Qu, Highly ordered supramolecular assembled networks tailored by bioinspired H-bonding confinement for recyclable ion-transport materials, CCS Chem. 5 (2023) 1422–1432.

[50] M. Valko, C. Rhodes, J. Moncol, M. Izakovic, M. Mazur, Free radicals, metals and antioxidants in oxidative stress-induced cancer, Chem. Biol. Interact. 160 (2006) 1–40.
[51] L. Packer, E. Witt, H. Tritschler, Alpha-lipoic acid as a biological antioxidant, Free Radic. Biol. Med. 19 (1995) 227–250.
[52] Y. Deng, Q. Zhang, B. Feringa, H. Tian, D. Qu, Toughening a self-healable supramolecular polymer by ionic cluster-enhanced iron-carboxylate complexes, Angew. Chem. Int. Ed. 59 (2020) 5278–5283.
[53] C. Cai, S. Wu, Z. Tan, F. Li, S. Dong, On-site supramolecular adhesion to wet and soft surfaces via solvent exchange, ACS Appl. Mater. Interfaces 13 (2021) 53083–53090.
[54] J. Zhao, Y. Wei, J. Xiong, H. Liu, G. Lv, J. Zhao, H. He, J. Gou, T. Yin, X. Tang, Y. Zhang, Antibacterial-anti-inflammatory-bone restoration procedure achieved by MIN-loaded PLGA microsphere for efficient treatment of periodontitis, AAPS PharmSciTech 24 (2023) 74.
[55] W. Zhou, Y. Du, X. Li, C. Yao, Lipoic acid modified antimicrobial peptide with enhanced antimicrobial properties, Bioorg. Med. Chem. 28 (2020) 115682.
[56] A. Gliga, S. Skoglund, I. Wallinder, B. Fadeel, H. Karlsson, Size-dependent cytotoxicity of silver nanoparticles in human lung cells: the role of cellular uptake, agglomeration and Ag release, Part. Fibre Toxicol. 11 (2014) 17.